Chapter III
Observational Data

In this work, we use information from many sources to study and compare the coronal magnetic loop structures of the Sun with our simulation results.

3.1 Total Solar Eclipse Photography from the Research Group of Chulalongkorn University

On October 24^{th} 1995, a total solar eclipse occurred in Thailand, which was a good chance for Thai people to see this event in many areas. In Thailand, a total solar eclipse will not be visible for at least another 75 years after that event. Therefore, astrophysicists interested in research about the Sun had only once chance in their lifetimes to observe and record this event from Thai soil. A group of scientists from Chulalongkorn University traveled to observe this event in Kampaeng Phet Province and obtained scientifically useful data (Figure 3.1) from observations using a telescope with a specially ordered narrow-band filter which only transmits light within a 5 Å bandwidth at wavelengths about 6374 Å, a wavelength emitted by Fe X (Fe^{+9}). The ion Fe^{+9} can only be found at a temperature close to 1.0×10^6 K (see Appendix A). This wavelength was also used by Hanaoka, Kurokawa, and Saito (1988) to observe the coronal loop structures above an active region during the total solar eclipse of February 16^{th}, 1980 in Kenya. They took three monochromatic images in Fe X λ6374 Å (1.0×10^6 K or

cool corona), Fe XIV λ5303 Å (2.0×10^6 K or medium-temperature corona) and continuum wavelengths. In 1991, Kurokawa, Kitai, and Ishiura observed the total solar eclipse of July 11^{th}, 1991 at La Paz, Mexico and high resolution pictures of the inner corona were successfully obtained in the Fe X, Fe XIV, Ca XV λ5694 Å(3.5×10^6 K), Hα lines (1.0×10^4 K), and continuum wavelengths (Kurokawa, Kitai, and Ishiura, 1995).

For our observation, a 4-inch telescope, with a camera, was mounted on a motorized rotating equatorial mount, which is important for high resolution photography. The research team had specially ordered two narrow band filters, green with a bandwidth of 5 Å centered at 5303 Å of Fe^{+13} and red with a similar bandwidth and a wavelength of about 6374 Å. Only the red filter was used, for a 25-second exposure an black-and-white film, because the Sun was covered by a cloud from 30 seconds after 2^{nd} contact until the end of the total eclipse. The first contact occurred at 9:17:47 AM, the 2^{nd} was at 10:44:42 AM, and the 3^{rd} and the 4^{th} were not recorded because of the clouds (for more details see Ruffolo, 1996).

From our photograph in Figure 3.1, we can see a high resolution image of a coronal magnetic loop structure in the coronal layer at the west of solar limb (upper right in Figure 3.1) which is not seen in white-light photographs. This shows that the plasma inside the loop has a lower temperature than most of the corona (Ruffolo, 1996). We can also see an apparent discontinuity in the plasma density in our picture, which may be caused by coronal activity occurring shortly before the solar eclipse. In this thesis, we simulated the magnetic field lines of the active region in order to compare with this image and other data which we will show in the next sections, to verify the magnetic field structure and apparent discontinuity. To our knowledge, such high-quality emission-line observations have been previously published by only one other group (Hanaoka,

Kurokawa, and Saito, 1988; Kurokawa, Kitai, and Ishiura, 1995) in the world (for other eclipses). Therefore, these data provide an important source of information on coronal loops.

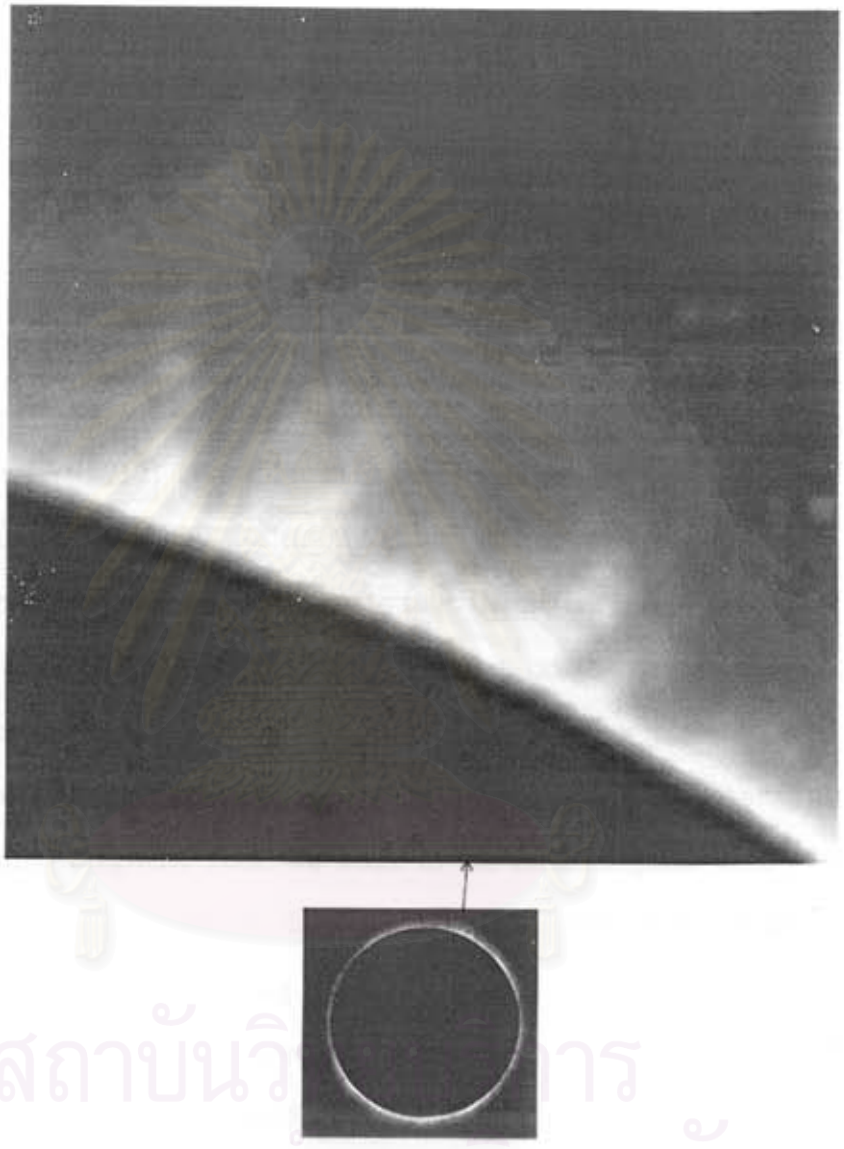

Figure 3.1: An enlarged version of figure 1.2, the Fe^{+9} image of the total solar eclipse on 24^{th} October, 1995 taken by a group of scientists from Chulalongkorn University at Klonglan National Park, Kampaeng Phet Province.

3.2 Data from Kitt Peak Magnetograms

Kitt Peak magnetogram images in Figures 3.2 - 3.6 show us the magnetic field component along the viewing direction on the solar disk using the Zeeman effect. In our work, we are only interested in an active region called AR7912 where is at a latitude of about 15° S, which included the magnetic loops observed during the solar eclipse, and we used these data as a boundary condition at $z = 0$ (on the solar surface) for simulating the coronal loop structures. On the pictures (figure 3.2 - 3.6), both the bright (emerging field) and dark (ingoing field) regions correspond to visible sunspots on the disk of opposite magnetic polarities.

It is important to examine data from several days in order to track the active region (AR7912) as it follows the Sun's rotation from East to West during the two weeks before the solar eclipse (the Sun's equatorial period is about 26 days). From these data we can estimate that the active region reached the West limb on or after October 22^{nd}, 1995. Therefore, on the day of the eclipse, the active region was actually behind the limb of the Sun.

Another reason for examining data from several days is that in estimating the coronal magnetic field, we want to use magnetogram data from a day close to the day of the eclipse, because we can see from these images that the active region is actually rotating internally, with the leading spot moving closer to the equator with time. However, data from October 20^{th} or 21^{st} contain substantial errors because of the surface elongation (greater length along the surface per pixel) near the limb, and because the line of sight is nearly tangent to the solar surface, so we are losing information about the outward component of **B**. Therefore, after trying to use data from different days, we decided on October 18^{th} as the best compromise and used these data as a boundary condition for our magnetic field modeling. These data were obtained from the WWW

(ftp://ftp.noao.edu/kpvt/daily/lowres/95.10), courtesy of the National Optical Astronomy Observatories (NOAO) as computer files in FITS format.

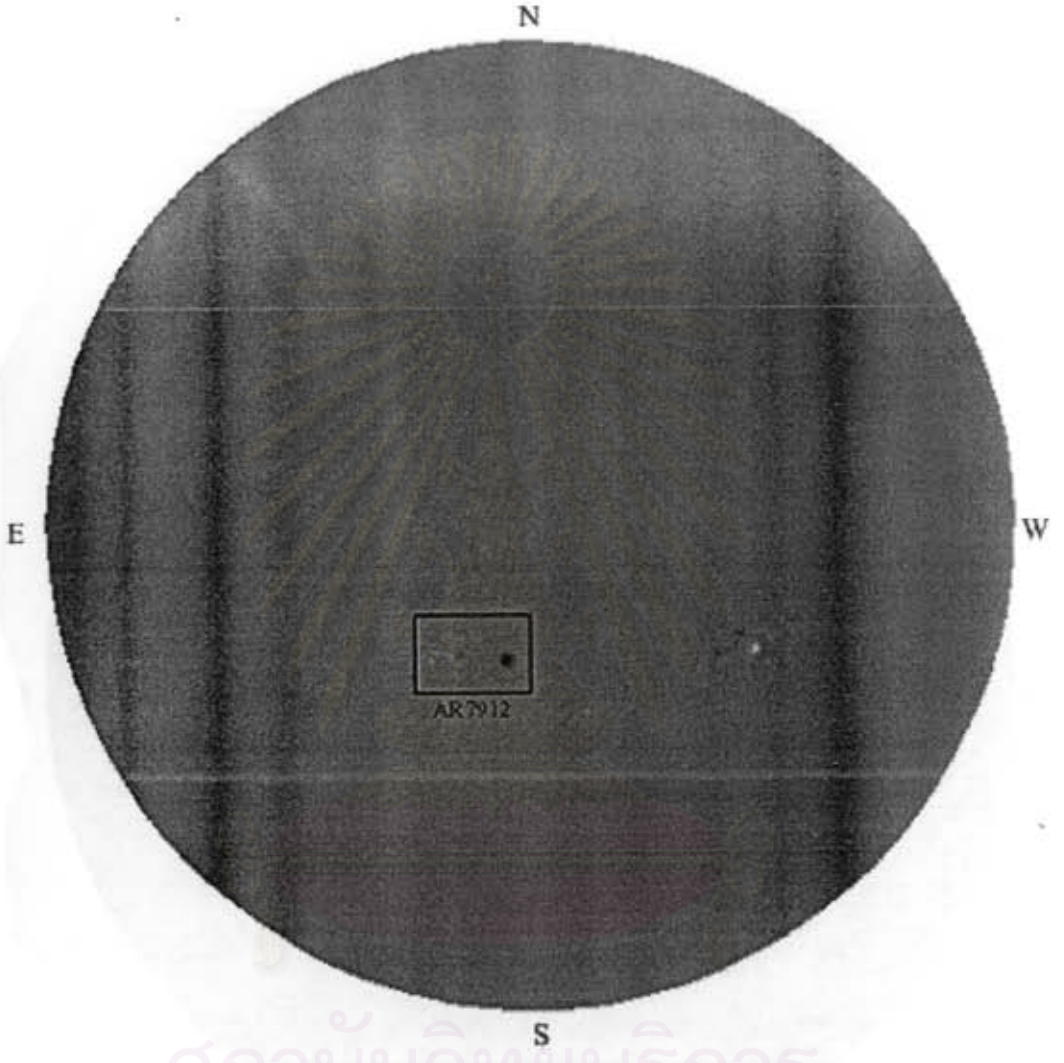

Figure 3.2: Full-disk photospheric distribution of the line-of-sight magnetic field component from the Kitt Peak magnetogram on October 15^{th}, 1995 (15:15:00 UT).

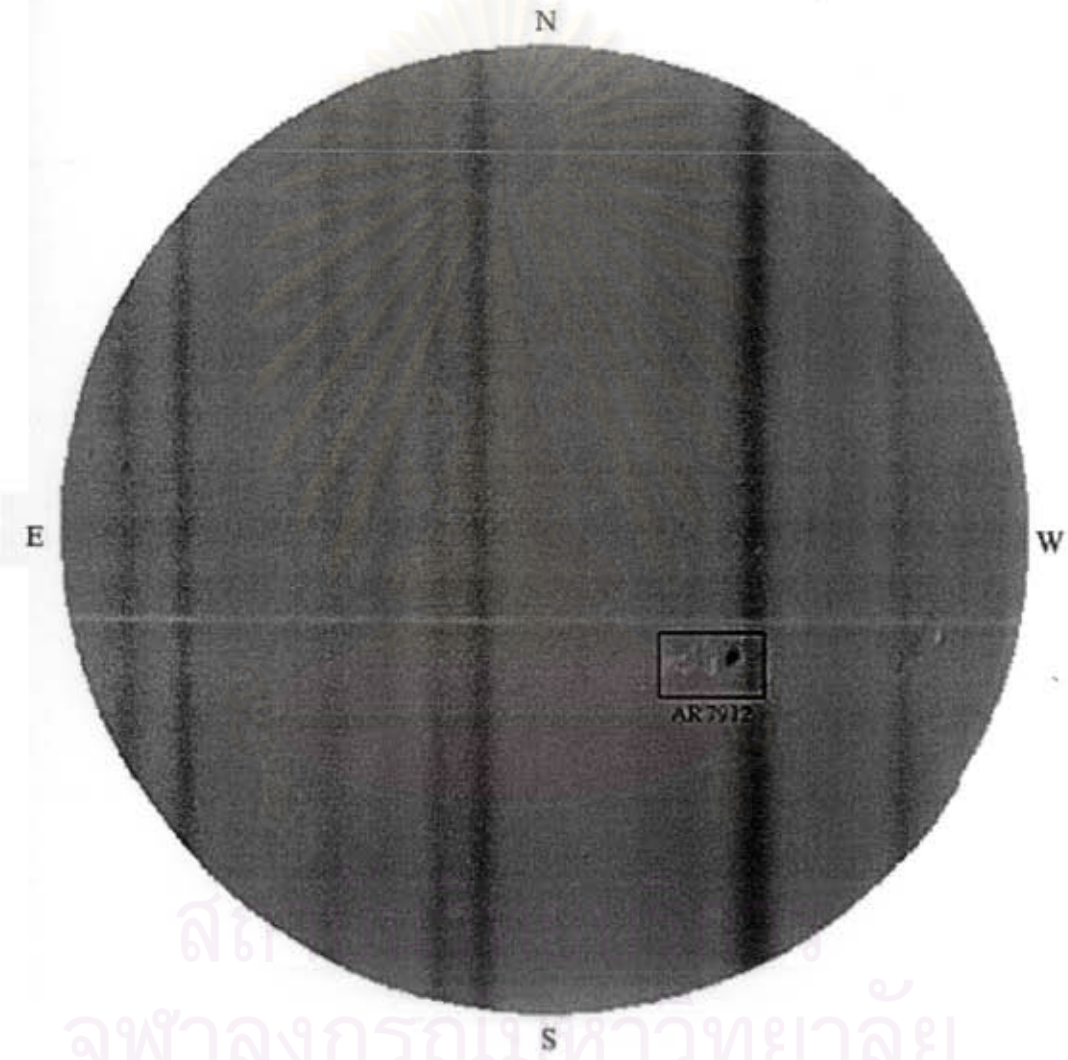

Figure 3.3: Full-disk photospheric distribution of the line-of-sight magnetic field component from the Kitt Peak magnetogram on October 17th, 1995 (15:34:47 UT).

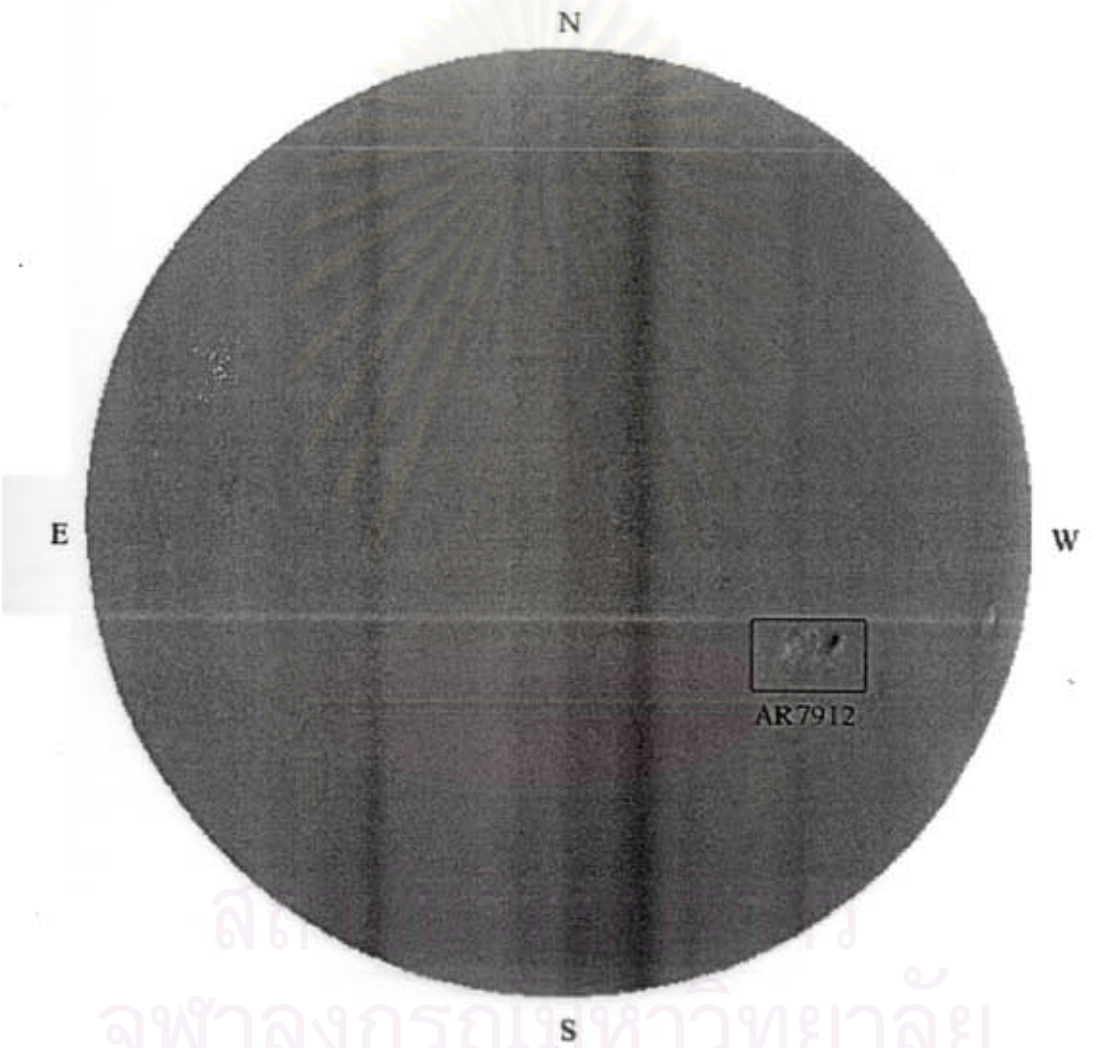

Figure 3.4: Full-disk photospheric distribution of the line-of-sight magnetic field component from the Kitt Peak magnetogram on October 18th, 1995 (14:59:24 UT).

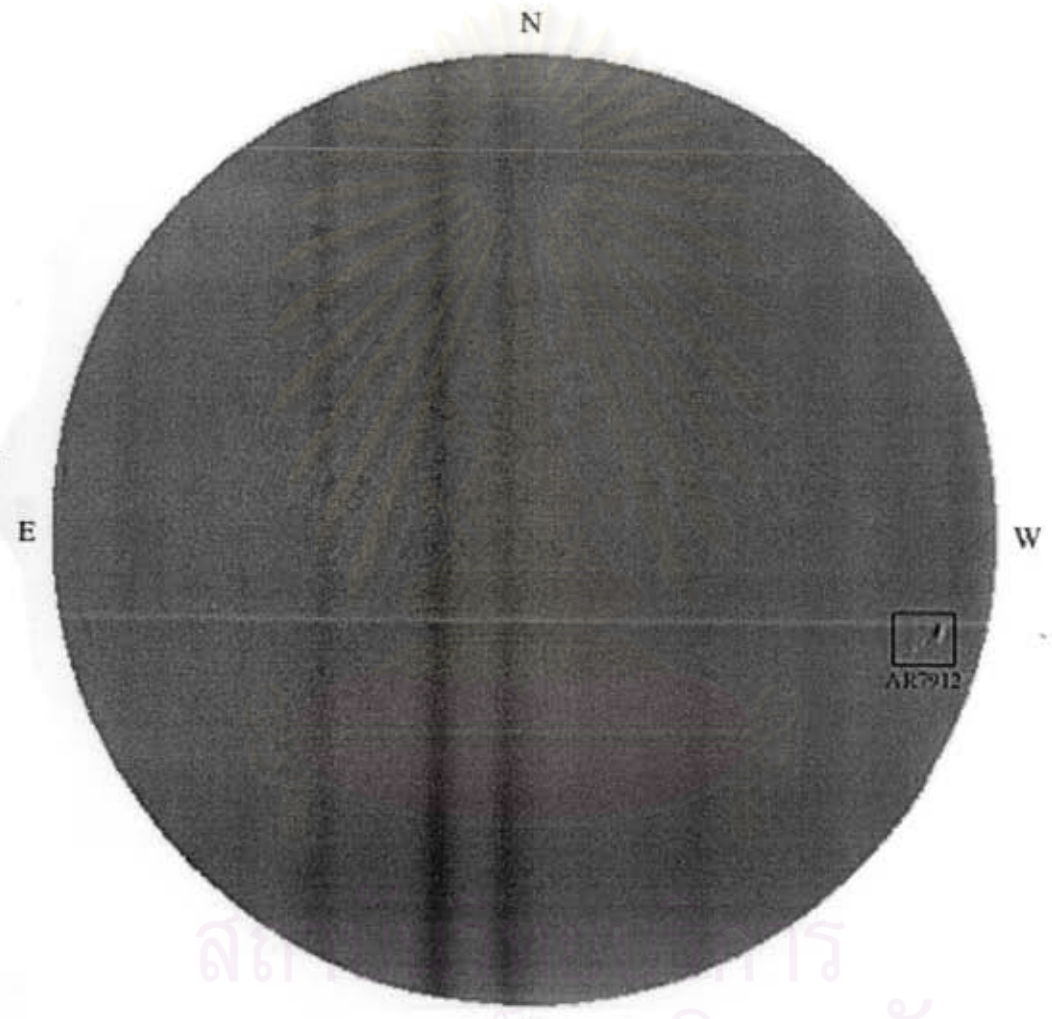

Figure 3.5: Full-disk photospheric distribution of the line-of-sight magnetic field component from the Kitt Peak magnetogram on October 20^{th}, 1995 (15:12:54 UT).

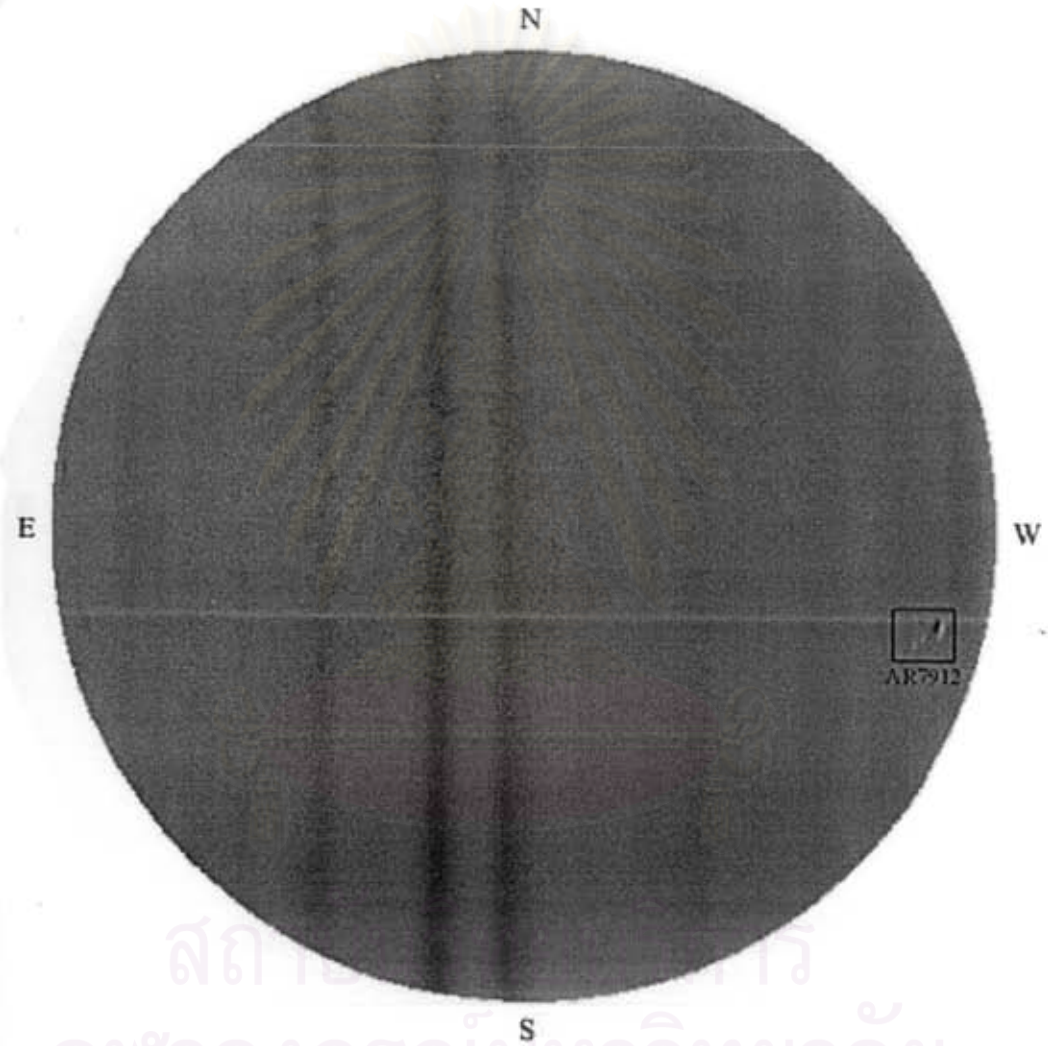

Figure 3.6: Full-disk photospheric distribution of the line-of-sight magnetic field component from the Kitt Peak magnetogram on October 21st, 1995 (15:40:12 UT).

3.3 X-ray Data from the Yohkoh Satellite

The X-ray images in Figures 3.7 - 3.10 also show us the magnetic network as we observe the density of high-temperature plasma on the disk. Note that these images confirm that on October 24^{th}, 1995, the day of the eclipse, AR7912 was already behind the West limb. The X-ray pictures show that three kinds of structures can be usefully distinguished. There are (1) magnetically closed loop structures of active regions, (2) the closed loops of quiet regions, whose footpoint separation is larger so the coronal magnetic intensity is lower, and (3) the open magnetic structures of coronal holes, where the field lines extend out into the solar wind and the mean field intensity is lowest. The X-ray-dark coronal structures indicate the closed coronal magnetic loops and bright areas indicate open magnetic field lines which are called coronal holes.

In the Figure 3.7 we saw the S-shape of region AR7912 that we are interested in, and we also used these data to visually compare with the results from the computational simulation of the magnetic loop structures to confirm our constant-α force-free condition and to indicate the most appropriate value of α.

Figure 3.7: X-ray image of the solar disk from the Yohkoh satellite on 17th October 1995 (04:42:47 UT).

Figure 3.8: X-ray image of the solar disk from the Yohkoh satellite on 20^{th} October 1995 (02:27:33 UT).

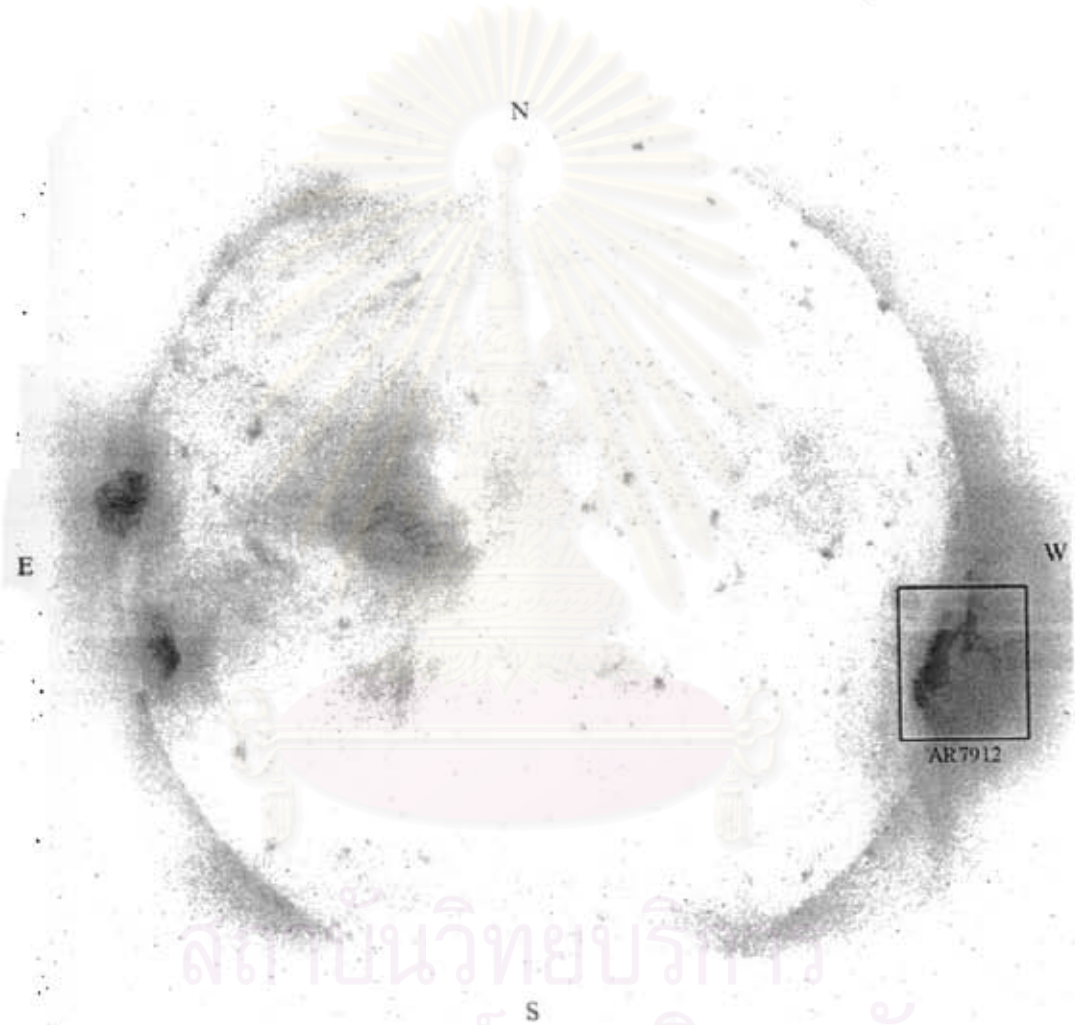

Figure 3.9: X-ray image of the solar disk from the Yohkoh satellite on 21st October 1995 (04:08:40 UT).

Figure 3.10: X-ray image of the solar disk from the Yohkoh satellite on 24^{th} October 1995 (08:39:46 UT).